1 October 1995

OPTICS COMMUNICATIONS

ELSEVIER

Optics Communications 120 (1995) 55–62

Determination of relative oscillator strengths by coherent Raman beats

Tilo Blasberg, Dieter Suter [1]

Institute of Quantum Electronics, ETH Zürich, CH-8093 Zürich, Switzerland

Received 24 April 1995

Abstract

Coherent Raman beats are transient phenomena that can be observed when a resonant test laser field undergoes coherent Raman scattering from a sublevel coherence that has been excited between two non-degenerate sublevels of an atom. It allows spectroscopic experiments on transitions between atomic sublevels with a resolution that is neither limited by the broadening of the optical transitions nor by the laser frequency jitter. While in most cases the theoretical description uses a three-level model atom, actual experiments involve multilevel atoms. In this article, we discuss effects that arise from the more complicated level structure for experiments that are performed on an inhomogeneously broadened ensemble of multilevel atoms. Using a pump-and-probe technique with a frequency-tunable probe laser beam, we investigate the relative oscillator strengths of the $^3H_4 \leftrightarrow {}^1D_2$ transitions of the impurity ion solid $Pr^{3+}:YAlO_3$. They depend on the relative orientation of the quantization axes in the ground and excited state. We compare the results of these purely optical experiments with data obtained earlier by optical–radio frequency double resonance methods.

1. Introduction

Coherent Raman scattering [1] occurs when a laser beam interacts with a resonant medium that contains a coherent excitation. This excitation can involve a vibrational transition [1], or it can be the coherent superposition of different spin states [2]. The main differences between coherent Raman scattering and spontaneous or stimulated Raman scattering are the dependence of the scattering cross section on the laser intensity and the phase relation between the exciting laser beam and the Raman field. In the case of coherent Raman scattering, the cross section is independent of the excitation intensity, i.e. the scattered field is directly proportional to the incident field [1]. This allows the observation of Raman scattering at low laser intensities. Moreover, the phase of the scattered field is locked to the phase of the incident field. The difference between both fields depends on the phase of the coherent excitation. The beat signal between the incident laser field and the scattered Raman field is therefore a faithful image of the coherent excitation.

In many experiments, the coherent superposition between two non-degenerate sublevels is excited continuously, e.g. with a resonant radiofrequency [3] or microwave field. In coherent Raman beat experiments, however, the sample preparation occurs before the actual detection period, in close analogy to nuclear magnetic resonance experiments [4]. The interference between the test laser field and the scattered Raman field on a quadratic photodetector gives rise to a beat

[1] Address after 1 October 1995: Universität Dortmund, Fachbereich Physik, D-44221 Dortmund, BRD; e-mail: suter@fuj.physik.uni-dortmund.de.

signal that oscillates at the Bohr frequency of the sublevel splitting. In addition, the signal contains information on dynamic interactions in the sample, since the sublevel coherence decays during the detection period. Due to this high information content, coherent Raman beats have found various applications in high-resolution spectroscopy of atomic [5,6] or molecular vapors [7,8]. Another important class of materials is rare-earth ions in crystals, where coherent Raman beats have been used to determine the splittings between individual nuclear spin substates [9,10].

Coherent Raman scattering requires an atomic V-type or Λ-type configuration with two allowed optical transitions that connect the two non-degenerate sublevels of one electronic state with a different electronic state. While the theoretical description of coherent Raman beats [2,11] has only considered three-level atoms, actual experiments use multilevel atoms. In these systems, coherent Raman scattering from a coherently excited sublevel transition can occur through all optical transitions that originate from one of the two states associated with the sublevel coherence. If an optical experiment on an inhomogeneously broadened ensemble of multilevel atoms uses a single laser beam, the total observable beat signal is the superposition of various signal contributions. As has been shown recently in the case of steady-state excitation [12], pump-and-probe techniques that use a frequency-tunable test laser field sometimes allow to separate these individual signal contributions.

This article discusses multilevel effects that were observed in coherent Raman beat experiments on the $^3H_4 \leftrightarrow {}^1D_2$ transition of the solid $Pr^{3+}:YAlO_3$ (Pr^{3+}:YAP; YAl perovskite). The separation of individual scattering pathways provides more information than the conventional experiment and allows us to determine the relative strengths of all optical transitions between the nuclear spin substates of the ground and excited state. In Pr:YAP, these oscillator strengths depend on the relative orientation of the quantization axes of the nuclear spin eigenfunctions in the two electronic states [13], whose unambiguous determination has been difficult.

The article is structured as follows. After a brief discussion of coherent Raman beats, we discuss coherent Raman scattering in multilevel atoms and derive the laser frequency dependence of the coherent Raman beat signal from the energy-level scheme of our system. We then present experimental data from the $^3H_4 \leftrightarrow {}^1D_2$ transition of Pr:YAP and compare them with theoretical data.

2. Coherent Raman beats

Fig. 1 illustrates the principle of coherent Raman beats for a V-type three-level atom consisting of an electronic ground state $|1\rangle$ and two non-degenerate sublevels $|2\rangle$ and $|3\rangle$ of the electronically excited state. The experiment consists of two distinct periods: During the initial preparation period, a coherent superposition between two sublevels of the atom is excited. After the end of this preparation period, the coherence ρ_{23}, represented by the wavy line between levels $|2\rangle$ and $|3\rangle$, evolves freely under the atomic Hamiltonian at the Bohr frequency, which is proportional to the splitting of the atomic eigenstates. During the subsequent detection period we monitor the sublevel coherence with a resonant test laser field, which couples one of the two sublevels, e.g. level $|3\rangle$, to a different electronic state, in this case to the electronic ground state $|1\rangle$. Through the resonant interaction, the test laser field transforms the initial superposition state between sublevels $|2\rangle$ and $|3\rangle$ into a new superposition state

$$c_2|\psi_2\rangle + c_3|\psi_3\rangle \underset{\omega_{13}}{\rightarrow} c_2|\psi_2\rangle + c_1|\psi_1\rangle + c_3|\psi_3\rangle, \qquad (1)$$

which, apart from the sublevel coherence, also contains coherence in the optical transition between the elec-

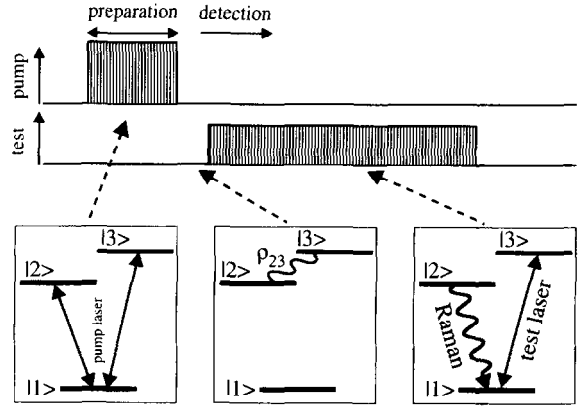

Fig. 1. Principle of coherent Raman beats. The experiment consists of a preparation period and a subsequent detection period, where a resonant test laser field is coherently Raman scattered from a sublevel coherence ρ_{23}.

tronic ground state $|1\rangle$ and the excited state sublevel $|2\rangle$. Macroscopically, this optical coherence corresponds to new electric dipoles, which are induced through the resonant interaction with test laser field. These dipoles contribute to the optical polarization of the sample

$$P = N \,\mathrm{Tr}(\rho\mu). \tag{2}$$

Here ρ denotes the density operator and μ represents the optical dipole operator. The new frequency component of the optical polarization is the source of the scattered Raman field $\mathscr{E}_R$ [2]

$$\mathscr{E}_R(L) = \mathrm{i}\,\frac{\omega_R^2 \mu_0}{2k} L P, \tag{3}$$

where μ_0 represents the magnetic permeability, k represents the wave vector, L is the length of the sample and ω_R is the angular frequency of the Raman field. The Raman field propagates together with the incident test laser field. On a quadratic photodetector the interference between the test laser field and the scattered Raman field causes a beat signal at the Bohr frequency of the sublevel coherence, which is not affected by an inhomogeneous broadening of the optical absorption of the sample.

The spectral power S of the Raman beat at the sublevel transition frequency, which follows from Eq. (3), is given by [2]

$$S \propto N E_0^2 |\mu_{12}\|\mu_{13}\|\rho_{23}|, \tag{4}$$

where μ_{12} and μ_{13} represent the transition matrix elements of the optical transitions $|1\rangle \leftrightarrow |2\rangle$ and $|1\rangle \leftrightarrow |3\rangle$, respectively, and ρ_{23} represents the sublevel coherence. The signal amplitude depends linearly on the power of the incident test laser beam ($\propto E_0^2$) and on the number N of atoms that interact with the test laser field. The signal is linear in the sublevel coherence and in the matrix elements of those optical transitions that are involved in the Raman scattering process.

As indicated by the energy-level scheme in Fig. 1, a prerequisite for coherent Raman scattering is an atomic V-type or Λ-type three-level configuration with two allowed optical transitions that connect the two nondegenerate sublevels of one electronic state with another electronic state. For the sample under consideration, Pr:YAP, these energy-levels represent different nuclear spin substates of either the electronic ground state or the electronically excited state. The coherent Raman scattering process itself can be considered as a transfer of coherence from a sublevel transition into an adjacent optical transition.

Since the signal amplitude is proportional to the sublevel coherence, an efficient excitation scheme is essential for the observation of coherent Raman beats. For this purpose we used a bichromatic pump laser field [14]. During the preparation period, each of its two frequency components are in resonance with one of the two optical transitions of the three-level atom, as indicated in Fig. 1. The simultaneous interaction of a three-level atom with two resonant laser fields induces a coherence in the sublevel transition. The bichromatic excitation scheme is much more efficient than the conventional monochromatic excitation, in particular when the sublevel frequency exceeds the optical Rabi frequency, which is of the order of tens of kHz in our experiment. In Ref. [10], we have derived an analytical expression for the sublevel coherence that is created by bichromatic pump laser pulses. We use this expression to compare the signal amplitudes of coherent Raman beats in different optical transitions.

3. Coherent Raman scattering in multilevel atoms

Coherent Raman scattering can only take place if the test laser field couples one of the two sublevels, which are involved in the sublevel transition, to a different electronic state. For a homogeneous ensemble of three-level atoms, this condition is only satisfied for two frequencies of the test laser beam, as shown in Fig. 2a. If the laser field with frequency ν_T, represented by the straight line, couples the ground state to the lower of the two excited states, the scattered Raman field, represented by the wavy line, has a frequency $\nu_T + \Delta$, i.e. it is anti-Stokes shifted. In the second case, the laser field couples to the energetically higher of the two sublevels, and the Raman field is Stokes-shifted. The theoretical stick spectrum at the bottom of Fig. 2a shows the resulting laser frequency-dependence of the coherent Raman beat signal. It consists of a doublet, whose two peaks arise from Stokes (full line) and anti-Stokes (dashed line) Raman scattering. The heights of the two peaks are identical [1], because identical optical transitions are involved in Stokes and anti-Stokes Raman scattering and hence the same transition matrix elements determine the signal amplitude in Eq. (4).

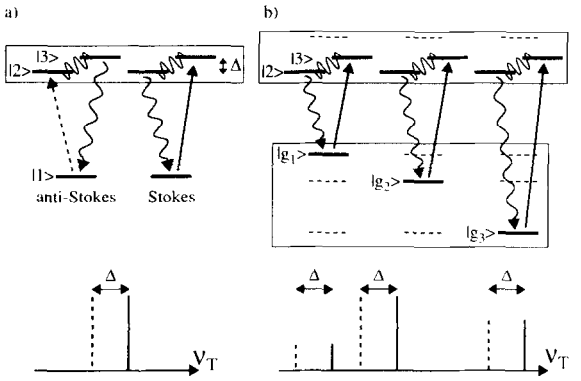

Fig. 2. Coherent Raman scattering from a coherence that has been excited between two non-degenerate sublevels of the excited state (a) assuming a three-level atom and (b) a multilevel atom with three non-degenerate sublevels of the electronic ground state. The bottom of the figure shows the dependence of the signal amplitude on the test laser frequency ν_T.

In most atoms, the electronic ground state consists of multiple sublevels and coherent Raman scattering can occur through different optical transitions. Fig. 2b illustrates this for the case of an atom with three non-degenerate ground state sublevels, with a coherent superposition present between two sublevels of the excited state. The laser frequency-dependence of the Raman signal now consists of three doublets. The amplitude of each resonance line is, according to Eq. (4), proportional to $|\mu_{g_i 2}\,\mu_{g_i 3}|$, where $|g_i\rangle$ labels the electronic ground state to which the test laser beam couples. Within each doublet, the lines have therefore identical intensities, but from doublet to doublet, the index i and therefore the signal amplitude changes. A comparison of the signal amplitudes for different test laser frequencies provides therefore information about the relative oscillator strengths of the atom.

If such an experiment is performed on real atoms, one has to cope with inhomogeneous broadening of the optical transitions. In a vapor, this broadening arises from Doppler shifts, in the solids that we use in our experiments, it is due to interactions with the crystal field. Because of crystal defects, this interaction varies with the position of the atoms. The resulting inhomogeneous line broadening exceeds the sublevel splittings by many orders of magnitude. If a single laser beam couples to such an ensemble of atoms, it can simultaneously be in resonance with all optical transitions for different subsets of atoms. On the other hand, if the pump laser beam that excites the coherent superposition in the medium is also a narrowband laser, it excites only those atoms that have a transition frequency close to the pump laser frequency. Like the test laser field, the pump laser field can couple any of the three ground state levels to the two excited state sublevels to excite the sublevel coherence ρ_{23}.

Only those atoms that are in resonance with the pump *and* test laser field can contribute to the Raman beat signal. To a good approximation, the total signal is therefore the superposition of those quasi-homogeneous sets of atoms that are excited by the pump laser field. For large enough inhomogeneous broadening, the signal depends not on the individual laser frequencies, but only on the frequency difference between the pump and test laser field. Fig. 3 summarizes the possible resonances. As shown in the left hand part, we assume that the ground state and the electronically excited state both consist of three sublevels. The pump laser beam that excites the sublevel coherence ρ_{23} contains two frequency components at frequencies $\nu_0 \pm \Delta/2$. The pump and test laser field can therefore simultaneously be in resonance with the same set of atoms, whenever the difference between the average pump laser frequency ν_0 and the test laser frequency ν_T matches an energy separation within the electronic ground state. The right hand part of Fig. 3 summarizes the nine pos-

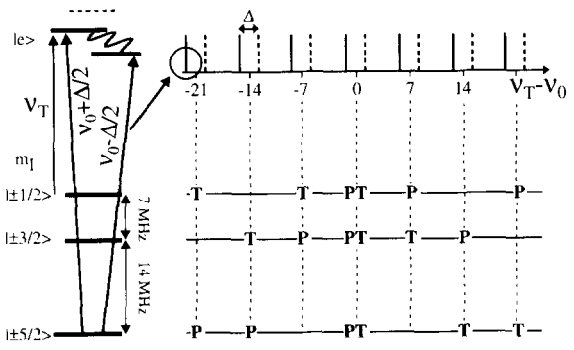

Fig. 3. The left-hand part shows the energy-level scheme of Pr:$YAlO_3$. A bichromatic pump laser field with center frequency ν_0 excites a sublevel coherence in the excited state. A test laser field with frequency ν_T is coherently Raman scattered from this sublevel coherence. The stick spectrum on the right-hand part shows schematically the dependence of the coherent Raman beat on the laser frequency difference. The letters P and T indicate those ground state sublevels, to which the pump (P) and test (T) laser field couple at the given laser frequency difference.

sible configurations that can contribute to the Raman beat signal.

The stick spectrum on the top of Fig. 3 shows the frequency differences at which we expect to find a Raman beat signal: seven doublets separated by the excited state splitting Δ, centered at the ground state splittings, which are of the order of 0, ± 7, ± 14, and ± 21 MHz for the solid Pr^{3+}:YAP. The lower part shows to which of the ground state sublevels the pump (P) and test laser field (T) couple at the given frequency difference. As in the case of a single atom, Stokes and anti-Stokes scattering lead to a doublet, whose two peaks are separated by the excited state sublevel splitting Δ. Three subsets of atoms contribute to the doublet in the center of the spectrum, where the mean frequency of the average pump laser frequency is equal to the test laser frequency, and both laser fields couple to the same ground state sublevel. Six additional doublets appear symmetrically on each side of this central doublet. For these doublets, the pump and test laser fields couple to different sublevels in the electronic ground state but to the same sublevels in the excited state. For the leftmost resonance line, the transitions to which the two laser fields couple are indicated in the energy level scheme at the left hand part of the figure.

4. System

Before we describe the experiments, we discuss the relevant energy-level scheme of Pr:YAP. The experiments were performed on the optical transition between the lowest crystal field states of the $^3H_4$ and $^1D_2$ multiplets. The nuclear quadrupole interaction [15]

$$\mathscr{H}_Q = D\,[I_z^2 - (I/3)(I+1) + (\eta/3)(I_x^2 - I_y^2)] \qquad (5)$$

results in a preferential orientation of the ^{141}Pr nucleus ($I = 5/2$) in the inhomogeneous electric field at the lattice site. It leads to three doubly degenerate nuclear spin eigenstates whose energy depends on the coupling constant D and the asymmetry parameter η. For a small asymmetry parameter, the eigenstates of the Hamiltonian are close to the eigenstates $|\pm 1/2\rangle$, $|\pm 3/2\rangle$ and $|\pm 5/2\rangle$ of the nuclear spin component I_z in the direction of the quantization axis. For Pr:YAP, the sublevel splittings are 7, 14 and 21 MHz in the electronic ground state and 0.9, 1.6 and 2.5 MHz in the electronically excited state.

To calculate the transition matrix element for an optical transition between the ground state $|\Psi_g\rangle$ and the excited state $|\Psi_e\rangle$, we separate the total wavefunction of both states into two parts $|\phi\rangle$ and $|\chi\rangle$ [13,16], which describe the electronic and the nuclear spin wave function, respectively:

$$\langle \Psi_g | \boldsymbol{\mu} \cdot \boldsymbol{E} | \Psi_e \rangle = \langle \phi_g | \boldsymbol{\mu} \cdot \boldsymbol{E} | \phi_e \rangle \langle \chi_g | \chi_e \rangle$$
$$= \mu_{ge} \langle \chi_g | \chi_e \rangle. \qquad (6)$$

Since the electronic part $\mu_{ge} = \langle \phi_g | \boldsymbol{\mu} \cdot \boldsymbol{E} | \phi_e \rangle$ of the transition matrix element is identical for all nine possible transitions of Pr:YAP, the *relative* oscillator strengths are only determined by the overlap integral $\langle \chi_g | \chi_e \rangle$ between two nuclear spin eigenfunctions.

If the quantization axes in both electronic states were identical, only transitions between identical spin states would be allowed. For Pr:YAP, however, the two quantization axes are rotated against each other by an angle β around the common principal X axis [16]. To calculate the overlap integral (6) between the nuclear spin eigenfunctions, one therefore has to rotate the eigenfunctions of one electronic state into the principal axis system of the other electronic state.

5. Experiments

Both the bichromatic excitation and the detection of the sublevel coherence require an accurate control of the frequencies of the pump and test laser beam. Fig. 4

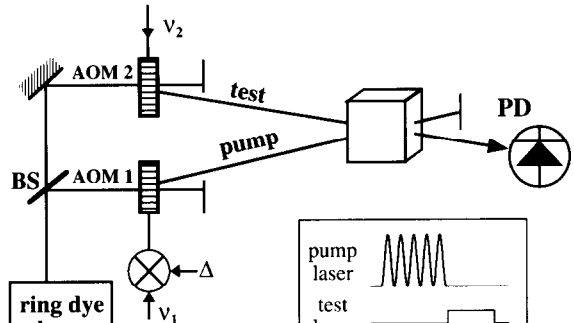

Fig. 4. Experimental setup. BS = beam splitter, AOM = acousto-optic modulators, ν_1, ν_2 and Δ = carrier and modulation frequency of the AOM driving signal, PD = photodiode. The inset shows the time dependence for the intensities of the pump and test laser beams.

illustrates how we implemented this control. The two acousto-optic modulators (AOM1 and AOM2) gate and frequency-shift the two laser beams, which originate from the same laser. To create the bichromatic pump laser field, the intensity of the pump laser pulses was modulated sinusoidally, resulting in two modulation sidebands. With the frequency of AOM1 held constant, the driving signal of AOM2 was varied to change the relative laser frequency difference. The two linearly polarized laser beams propagated along the crystallographic c-axis of the Pr:YAP crystal, intersecting at an angle of 5 mrad. Three orthogonal pairs of Helmholtz coils were used to cancel the earth magnetic field.

The insert in Fig. 4 illustrates the timing in the experiment. Typical durations for the pump laser pulses were of the order of 10 μs at laser intensities of 200–300 mW/mm^2. For an optimum signal amplitude, the modulation frequency Δ was in resonance with one of the sublevel transitions. After the end of the pump laser pulse, AOM2 switched on the weaker test laser beam (<1 mW/mm^2). The transmitted test laser field and the scattered Raman field propagated collinearly behind the crystal and interfered on a fast photodiode. To avoid the depletion of the nuclear spin populations of the electronic ground state by spectral hole-burning of the successive pump laser pulses, the two laser beams were switched off after each cycle, so that the system could relax towards thermal equilibrium before the subsequent pump pulse. In addition, the crystal temperature was set to 9 K to increase the nuclear spin relaxation rates [17]. The observed beat signal was Fourier transformed and the amplitude at the sublevel transition frequency Δ was measured as a function of the frequency difference between pump and test laser beam.

Fig. 5 shows the observed laser frequency-dependence of all three coherent Raman beat signals associated with the excited state of Pr:YAP ($\Delta = 0.92$, 1.56 and 2.48 MHz). The circles represent the experimental data, whereas the lines indicate the result of a numerical calculation that we discuss below. As expected from Fig. 3, each spectrum consists of seven doublets. The width of each resonance line corresponds to twice the laser frequency jitter (500 kHz), because two laser fields are involved in the excitation and the detection of the signal. Since the sublevel splittings in the excited state of Pr:YAP are of the same order of magnitude as the linewidth, the individual resonance lines could only be resolved for the largest splitting ($\Delta = 2.48$ MHz). The center frequency of each doublet corresponds to one of the ground state sublevel splittings (7.05, 14.1 or 21.15 MHz).

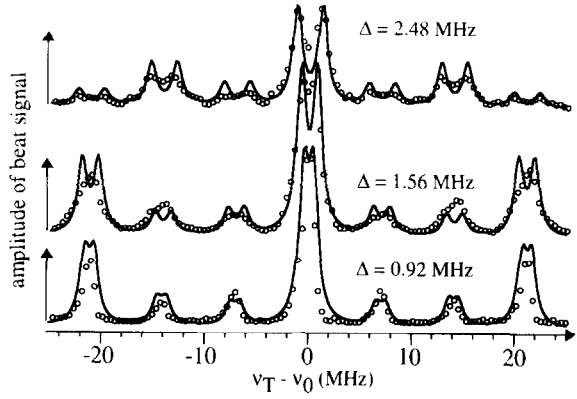

Fig. 5. Laser frequency dependence of all three coherent Raman beats that can be excited among the three excited state sublevels of Pr:YAP. The experimental data (points) are compared to theoretical spectra (lines).

6. Relative oscillator strengths

To extract the information on the relative oscillator strengths, we will next compare the observed laser frequency dependence (Fig. 5) with theoretical data. According to Eq. (6), the signal amplitude is proportional to the amplitude of the sublevel coherence. As we have shown previously [10], the sublevel coherence after a pulse length τ is given by

$$\rho_{23}(t) = \frac{\Omega_{12}\Omega_{13}}{\Omega_{12}^2+\Omega_{13}^2} \sin^2\left(\tfrac{1}{2}\sqrt{\Omega_{12}^2+\Omega_{13}^2}\,\tau\right). \tag{7}$$

Here Ω_{ij} denotes the optical Rabi-frequency of the transition $|i\rangle \leftrightarrow |j\rangle$

$$\Omega_{ij} = \mu_{ij}\mathscr{E}_0/\hbar \tag{8}$$

and ρ_{23} is the off-diagonal element of the density matrix that represents the sublevel coherence. The optical transitions that contribute to each resonance line were summarized in Fig. 3.

The relative oscillator strengths of the optical transitions between nuclear spin substates of different electronic states depend on the relative orientation of the quantization axes of the nuclear spin eigenfunctions.

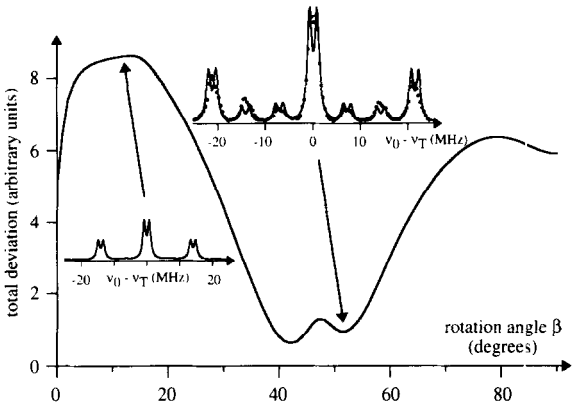

Fig. 6. Sum of the differences between the calculated and observed signal amplitudes for $\Delta = 0.92$ MHz and $\Delta = 1.56$ MHz as a function of the rotation angle β between the quantization axes of the nuclear spin eigenfunctions in the ground and excited state of Pr:YAP. The two insets show the laser frequency dependence for the two rotation angles quoted in the literature.

We treat this rotation angle as a parameter and calculate the eigenfunctions of the nuclear spin Hamiltonian (5) as a function of β. The nine relative transition matrix elements were calculated as the overlap between the nuclear spin eigenfunctions and inserted into Eqs. (7) and (4), assuming a pulse length of $\tau = 3$ μs and an optical Rabi frequency of 40 kHz for the most intense optical transition. The theoretical signal amplitudes of the seven doublets were then compared to the experimental data points. In Fig. 6, we plot the sum of the differences between theoretical and experimental data for $\Delta = 0.92$ MHz and $\Delta = 1.56$ MHz as a function of the rotation angle β. The total error clearly shows a double-minimum near $\beta = 47 \pm 5$ degrees.

The relative orientation of the nuclear quadrupole tensors of Pr:YAP has been determined previously. Experimental techniques included the observation of anti-crossings in the presence of an external magnetic field ($\beta = \pm 16.5°$ [18]) and measuring the dependence of the Raman heterodyne spectra on the orientation of an external magnetic field ($\beta = \pm 12.8°$ [16]). Another experiment, which considered the modulation of stimulated photon echos [19], could only reach a consistent interpretion of the experimental results by assuming a significantly larger angle of 40–60°. We assessed this controversy in a recent experiment [20] using Raman heterodyne spectroscopy in a small magnetic field of variable orientation, in combination with spectral holeburning. We found that the reason for the discrepancies is that the Pr^{3+}-ions occupy two non-equivalent lattice sites in the $YAlO_3$ host lattice, whose quadrupole tensors have different orientations. The magnetic resonance experiments [16,18] allow the determination of the tensor orientation, but not the assignment to the two lattice sites. Optical experiments, like spectral holeburning [20], photon echoes [19], and coherent Raman beats, however, depend on the *relative* orientation and can therefore be used to determine which of the two orientations correspond to the same lattice sites. The two possibilities correspond to $\beta = \pm 12.2°$, which is similar to the two earlier experiments, or to $\beta = \pm 55.0°$.

For both rotation angles, the two insets in Fig. 6 show the theoretical laser frequency dependence of the coherent Raman beat signal at $\Delta = 1.56$ MHz. In both spectra, the individual resonance lines were approximated by Lorentzian line shapes with a FWHM = 1 MHz. For the smaller rotation angle, we expect only three doublets, which is clearly inconsistent with the experiment. For the larger rotation angle, however, where state mixing allows Raman scattering through all optical transitions, the calculated data fit the experimental ones reasonably well. The laser frequency-dependence of the coherent Raman beat favors therefore the larger rotation angle. This relative orientation of the quadrupole tensors results in a new set of optical transition matrix elements and has therefore implications on virtually all optical experiments that are performed on the $^3H_4 \leftrightarrow {}^1D_2$ transition of Pr:YAP.

7. Conclusion

In this article we have discussed the observation of coherent Raman beats in multilevel atoms. For inhomogeneously broadened optical transitions, coherent Raman scattering can take place in various optical transitions. To separate these signal contributions, we have used a pump-and-probe technique, with two independently frequency-tunable laser fields. With this technique one can obtain additional spectroscopic information on the sample, e.g. on the relative oscillator strengths. In contrast to magnetic resonance methods, the purely optical pump-and-probe technique yields an unambiguous result for the relative orientation of the

nuclear quadrupole tensors in the ground and excited state of Pr^{3+}:$YAlO_3$.

Acknowledgements

We gratefully acknowledge financial support by the Schweizerischer Nationalfonds.

References

[1] J.A. Giordmaine and W. Kaiser, Phys. Rev. 144 (1966) 676.
[2] R.G. Brewer and E.L. Hahn, Phys. Rev. A 8 (1973) 464.
[3] N.C. Wong, E.S. Kintzer, J. Mlynek, R.G. DeVoe and R.G. Brewer, Phys. Rev. B 28 (1983) 4993.
[4] R.R. Ernst and W.A. Anderson, Rev. Sci. Instrum. 37 (1966) 93.
[5] H. Burggraf, M. Kuckartz and H. Harde, Observation of 517 GHz fine-structure quantum-beats in Na, in: Methods of Laser Spectroscopy, eds. Y. Prior, A. Ben-Reuven and M. Rosenbluh (Plenum, New York, 1986).
[6] R.G. DeVoe and R.G. Brewer, Phys. Rev. Lett. 40 (1978) 862.
[7] J.P. Heritage, T.K. Gustafson and C.H. Lin, Phys. Rev. Lett. 34 (1975) 1299.
[8] A.Z. Genack and R.G. Brewer, Phys. Rev. A 17 (1978) 1463.
[9] R.M. Shelby, A.C. Tropper, R.T. Harley and R.M. Macfarlane, Optics Lett. 8 (1983) 304.
[10] T. Blasberg and D. Suter, Phys. Rev. B 51 (1995) 6309.
[11] R.G. Brewer and E.L. Hahn, Phys. Rev. A 11 (1975) 1641.
[12] T. Blasberg and D. Suter, Phys. Rev. B 51 (1995).
[13] R.M. MacFarlane and R.M. Shelby, Coherent transient and holeburning spectroscopy of rare earth ions in solids, in: Spectroscopy of Solids Containing Rare Earth Ions, eds. A. Kaplyanskii and R.M. MacFarlane (North-Holland, Amsterdam, 1987).
[14] T. Blasberg and D. Suter, Optics Comm. 109 (1994) 133.
[15] M.H. Cohen and F. Reif, Solid State Physics 5 (1957) 321.
[16] M. Mitsunaga, E.S. Kintzer and R.G. Brewer, Phys. Rev. B 31 (1985) 6947.
[17] T. Blasberg and D. Suter, Chem. Phys. Lett. 215 (1993) 668.
[18] A. Wokaun, S.C. Rand, R.G. DeVoe and R.G. Brewer, Phys. Rev. B 23 (1981) 5733.
[19] M. Mitsunaga, R. Yano and N. Uesugi, Phys. Rev. B 45 (1992) 12760.
[20] T. Blasberg and D. Suter, Determination of oscillator strenghts in Pr^{3+}:$YAlO_3$ by Raman heterodyne and hole burning spectroscopy, J. Luminesc., in print.